

Platinum(0) Complexes of Chiral Diphosphines: Enantioface-Selective Binding of *trans*-Stilbene

Denyce K. Wicht, Michael A. Zhuravel, Ronald V. Gregush, and David S. Glueck*

6128 Burke Laboratory, Department of Chemistry, Dartmouth College, Hanover, New Hampshire 03755

Ilia A. Guzei, Louise M. Liable-Sands, and Arnold L. Rheingold

Department of Chemistry, University of Delaware, Newark, Delaware 19716

Received November 13, 1997

The zerovalent complexes Pt(diphos)(*trans*-stilbene) (diphos = dppe, dppf, (*S,S*)-Chiraphos, *R*-Tol-Binap, (*R,R*)-Me-Duphos, (*S,S*)-Diop) were prepared by reduction of the corresponding Pt(diphos)Cl₂ compounds. NMR and crystal structure data show that the *trans*-stilbene complexes with chiral diphosphines exist as a mixture of diastereomers differing in their binding of the enantiofaces of the prochiral olefin; for *R*-Tol-Binap, they can be separated by recrystallization. The complexes Pt((*R,R*)-Me-Duphos)Cl₂ and Pt(diphos)(*trans*-stilbene) (diphos = dppf, (*S,S*)-Chiraphos, *R*-Tol-Binap, (*S,S*)-Diop) were structurally characterized by X-ray crystallography.

Introduction

Zerovalent platinum complexes are useful starting materials for studies of oxidative addition and its role in catalysis.¹ Analogous chiral reagents find applications in asymmetric synthesis.² Our interest in platinum-catalyzed hydrophosphination³ and a possible asymmetric version of this reaction led us to investigate sources of the Pt(diphos) fragment (diphos = bidentate diphosphine) as catalyst precursors.⁴ The ethylene compounds⁵ PtL₂(C₂H₄) are common reagents, but related *trans*-stilbene complexes⁶ are, in general, easier to prepare and more robust.⁷ We report here the synthesis of a series of Pt(diphos)(*trans*-stilbene) complexes and NMR and crystallographic studies of chiral recognition of the *trans*-stilbene enantiofaces by chiral Pt(diphos) fragments.

Gladysz and Boone have recently reviewed the literature on molecular recognition in related π -complexes of chiral metal moieties.⁸ The Pt(0) complex Pt(Diop)-(C₂H₄) has been used as a chiral derivatizing agent to assay the enantiomeric excess of racemic mixtures of olefins and to study enantioface recognition of prochiral olefins.⁹ Here, we report investigations of the coordination of one substrate, *trans*-stilbene, to a series of related chiral metal fragments. In contrast, binding of a variety of structurally related ligands to the same chiral metal center has often been examined.¹⁰

Results and Discussion

The precursors Pt(diphos)Cl₂ were prepared from Pt-(COD)Cl₂ (COD = 1,5-cyclooctadiene) and the appropriate diphosphine.¹¹ The (*R,R*)-Me-Duphos and *R*-Tol-Binap complexes **1** and **2** are new and were characterized spectroscopically and by elemental analyses.¹² In ad-

(1) (a) Collman, J. P.; Hegedus, L. S.; Norton, J. R.; Finke, R. G. *Principles and Applications of Organotransition Metal Chemistry*; University Science Books: Mill Valley, CA, 1987. (b) Parshall, G. W.; Ittel, S. D. *Homogeneous Catalysis: the Applications and Chemistry of Catalysis by Soluble Transition Metal Complexes*, 2nd ed.; Wiley: New York, 1992.

(2) Noyori, R. *Asymmetric Catalysis in Organic Synthesis*; Wiley-Interscience: New York, 1994.

(3) Wicht, D. K.; Kourkine, I. V.; Lew, B. M.; Nthenge, J. M.; Glueck, D. S. *J. Am. Chem. Soc.* **1997**, *119*, 5039–5040.

(4) For related studies, see: (a) Brown, J. M.; Perez-Torrente, J. J.; Alcock, N. W. *Organometallics* **1995**, *14*, 1195–1203. (b) Paganelli, S.; Matteoli, U.; Scriveranti, A. *J. Organomet. Chem.* **1990**, *397*, 119–125.

(5) (a) Head, R. A. *Inorg. Synth.* **1990**, *28*, 132–135. (b) Blake, D. M.; Roundhill, D. M. *Inorg. Synth.* **1978**, *18*, 120–125. (c) Camalli, M.; Caruso, F.; Chaloupka, S.; Leber, E. M.; Rimml, H.; Venanzi, L. M. *Helv. Chim. Acta* **1990**, *73*, 2263–2274. (d) Nagel, U. *Chem. Ber.* **1982**, *115*, 1998–1999. (e) Smith, V. C. M.; Aplin, R. T.; Brown, J. M.; Hursthouse, M. B.; Karalulov, A. I.; Malik, K. M. A.; Cooley, N. A. *J. Am. Chem. Soc.* **1994**, *116*, 5180–5189. (f) Brown, J. M.; Cooley, N. A. *Organometallics* **1990**, *9*, 353–359.

(6) Some complexes PtL₂(*trans*-stilbene) are known for monodentate phosphines L. (a) PPh₃; Chatt, J.; Shaw, B. L.; Williams, A. A. *J. Chem. Soc. A* **1962**, 3269–3270. (b) PEt₃; Browning, J.; Green, M.; Spencer, J. L.; Stone, F. G. A. *J. Chem. Soc., Dalton Trans.* **1974**, 97–101. (c) PMe₃; Green, M.; Spencer, J. L.; Stone, F. G. A.; Welch, A. J. *J. Chem. Soc., Dalton Trans.* **1975**, 179–184.

(7) (a) For example, the procedure for generation of a variety of PtL₂-(C₂H₄) complexes (ref 5a) states that they cannot be isolated by removing the solvent. (b) Lesley, G.; Nguyen, P.; Taylor, N. J.; Marder, T. B.; Scott, A. J.; Clegg, W.; Norman, N. C. *Organometallics* **1996**, *15*, 5137–5154. Reference 9 describes the isolation of ethylene complexes of Pt(dppe) and dppb (dppe = Ph₂P(CH₂)₂PPh₂, dppb = Ph₂P(CH₂)₄PPh₂), but these were not obtained pure (see p 5139). (c) Brown, J. M.; Cook, S. J.; Kimber, S. J. *J. Organomet. Chem.* **1984**, *269*, C58–C60. Pt(dppb)(C₂H₄) was prepared by reduction of the dichloride with NaBH₄ in CH₂Cl₂/EtOH under ethylene, but the dppp analogue (dppp = Ph₂P(CH₂)₃PPh₂) made in this way was contaminated with Pt(dppp)₂. (d) Reference 4a states (p 1196) that Pt-(Chiraphos)(C₂H₄) could not be prepared by NaBH₄ reduction of Pt(Chiraphos)Cl₂ under ethylene.

(8) Gladysz, J. A.; Boone, B. J. *Angew. Chem., Int. Ed. Engl.* **1997**, *36*, 550–583.

(9) See Scheme 1 for the structure of Diop. (a) Reference 7c (b) Parker, D.; Taylor, R. J. *J. Chem. Soc., Chem. Commun.* **1987**, 1781–1783. (c) Parker, D.; Taylor, R. J. *Tetrahedron* **1988**, *44*, 2241–2248. (d) Fulwood, R.; Parker, D.; Ferguson, G.; Kaltner, B. *J. Organomet. Chem.* **1991**, *419*, 269–276.

(10) See refs 8 and 9 and for a recent example: Quan, R. W.; Li, Z.; Jacobsen, E. N. *J. Am. Chem. Soc.* **1996**, *118*, 8156–8157.

Table 1. Crystallographic Data for 1, 4–6, and 8

	1	4	5	6	8
formula	C ₁₉ H ₃₀ Cl ₄ P ₂ Pt	C ₅₂ H ₄₈ FeOP ₂ Pt	C ₄₆ H ₄₈ OP ₂ Pt	C ₆₆ H ₆₀ OP ₂ Pt	C ₄₅ H ₄₄ O ₂ P ₂ Pt
fw	657.26	1001.78	873.97	1126.17	873.92
space group	P2 ₁ 2 ₁ 2 ₁	P2 ₁ /n	I222	P2 ₁ 2 ₁ 2 ₁	P $\bar{1}$
a, Å	9.7798(2)	14.701(9)	16.8401(2)	11.0429(2)	12.5542(2)
b, Å	13.5498(2)	17.195(7)	25.4756(2)	16.4825(3)	14.2110(2)
c, Å	18.2175(3)	17.739(5)	37.1463(3)	28.8459(4)	14.3244(2)
α , deg					75.6220(6)
β , deg		94.67(3)			68.8019(7)
γ , deg					70.4527(7)
V, Å ³	2414.08(5)	4469(4)	15936.18(12)	5250.38(15)	2221.64(8)
Z	4	4	16	4	2
cryst color, habit	colorless block	red block	yellow plate	yellow plate	yellow block
D(calc), g cm ⁻³	1.808	1.489	1.427	1.425	1.409
μ (Mo K α), cm ⁻¹	63.91	35.60	36.34	27.77	32.68
temp, K	173(2)	257(2)	223(2)	213(2)	213(2)
abs corr	empirical		empirical		empirical
T(max)/T(min)	1.000/0.376		1.000/0.420		1.000/0.781
diffractometer	P4/CCD	Siemens P4	P4/CCD	P4/CCD	P4/CCD
radiation			Mo K α (λ = 0.710 73 Å)		
R(F), % ^a	2.53	6.28	3.87	2.98	4.68
R(wF ²), % ^a	6.09	12.53	10.00	6.14	12.87

^a Quantity minimized = $R(wF^2) = \sum [w(F_o^2 - F_c^2)^2] / \sum [(wF_o^2)^2]^{1/2}$; $R = \sum \Delta / \sum (F_o)$, $\Delta = |F_o - F_c|$.

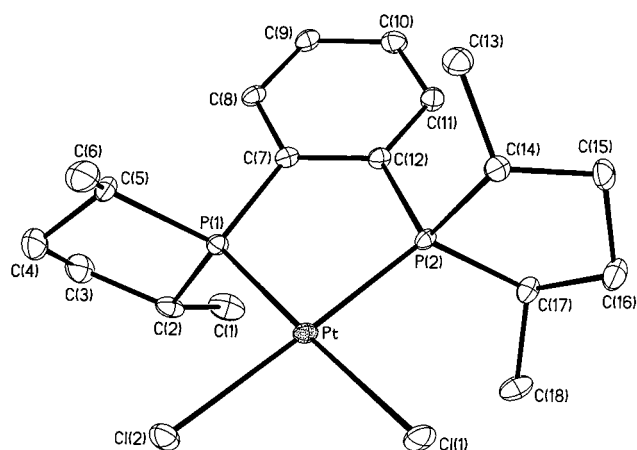
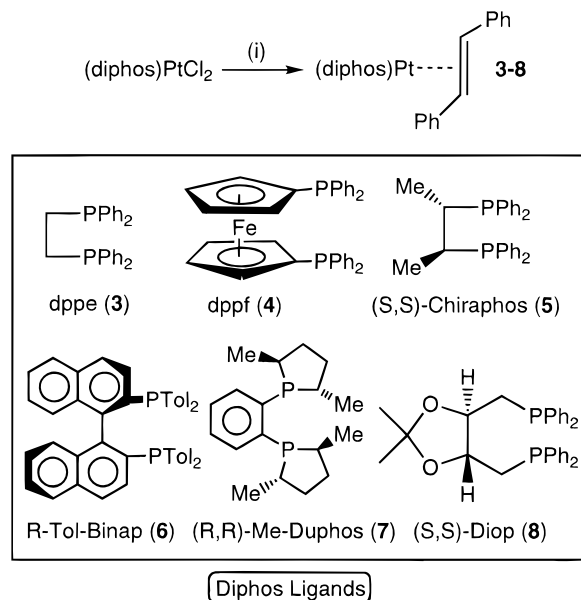


Figure 1. ORTEP diagram of **1**·CH₂Cl₂, with 30% probability thermal ellipsoids. The solvent molecule is not shown. Selected bond lengths (Å): Pt–P(2) 2.2178(13), Pt–P(1) 2.2183(11), Pt–Cl(1) 2.3828(12), Pt–Cl(2) 2.3881(12). Selected bond angles (deg): P(2)–Pt–P(1) 87.73(4), P(2)–Pt–Cl(1) 89.72(5), P(1)–Pt–Cl(1) 177.20(5), P(2)–Pt–Cl(2) 177.91(5), P(1)–Pt–Cl(2) 90.21(4), Cl(1)–Pt–Cl(2) 92.34(4).

dition, the Duphos complex **1** was structurally characterized by X-ray crystallography as a CH₂Cl₂ solvate. Data collection and structure refinement are summarized in Table 1. An ORTEP diagram and selected bond lengths and angles appear in Figure 1, and additional information is in the Experimental Section and the Supporting Information. The complex adopts the expected square-planar structure. The Duphos bite angle is 87.73(4)°; this small distortion is balanced by the Cl–Pt–Cl angle of 92.34(4)°. The Pt–Cl bond

(11) See Scheme 1 for ligand structures. Most of these dichlorides have been reported previously. dppe: Hudson, M. J.; Nyholm, R. S.; Stiddard, M. H. B. *J. Chem. Soc. A* **1968**, 40–43. dppf: Bandini, A. L.; Banditelli, G.; Cinellu, M. A.; Sanna, G.; Minghetti, G.; Demartin, F.; Manassero, M. *Inorg. Chem.* **1989**, *28*, 404–410 and ref 1 therein. Chiraphos: Morandini, F.; Consiglio, G.; Piccolo, O. *Inorg. Chim. Acta* **1982**, *57*, 15–19. Diop: Gramlich, V.; Consiglio, G. *Helv. Chim. Acta* **1979**, *62*, 1016–1024.

(12) The closely related Pt(S–Binap)Cl₂ has been prepared (Kollar, L.; Sandor, P.; Szalontai, G. *J. Mol. Catal.* **1991**, *67*, 191–198) and shows $^1J_{Pt-P} = 3667$ Hz.

Scheme 1^a

^a (i) Reagents: *trans*-stilbene + 2 equiv of reducing agent; LiEt₃BH for **3–5**, NaBH₄ for **6**, NaBH(OMe)₃ for **7** and **8**.

lengths (2.383(12) and 2.388(12) Å) are similar to those for *cis*-Pt(PMe₃)₂Cl₂ (2.364(8) and 2.388(9) Å),¹³ consistent with similar *trans* influences for PMe₃ and Duphos.

The Pt(0) *trans*-stilbene complexes **3–8** (diphos = dppe (**3**), dppf (**4**), (*S,S*)-Chiraphos (**5**), *R*-Tol-Binap (**6**), (*R,R*)-Me-Duphos (**7**), (*S,S*)-Diop (**8**)) were prepared by reduction of the corresponding dichlorides in the presence of excess *trans*-stilbene (Scheme 1). An attempt to make Pt(dppe)(*cis*-stilbene) (**9**) initially gave the desired complex, according to ³¹P NMR monitoring of the reaction mixture, but isomerization occurred on workup and recrystallization to give a mixture of the *cis*- and *trans*-stilbene complexes **9** and **3**. When an isolated sample of this mixture is redissolved, further isomerization occurs slowly at room temperature; heating to 50 °C causes complete conversion of **9** into **3**.

(13) Messmer, G. G.; Amma, E. L.; Ibers, J. A. *Inorg. Chem.* **1967**, *6*, 725–730.

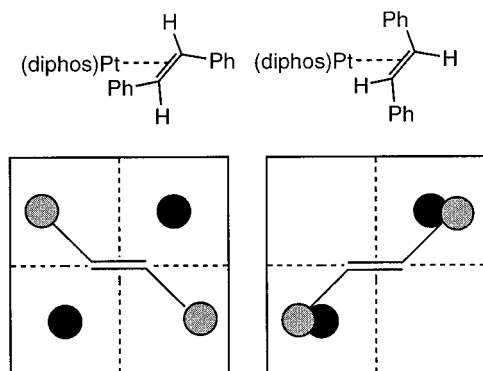


Figure 2. Two possible diastereomers of Pt(diphos)(*trans*-stilbene) (diphos = chiral bidentate diphosphine). The quadrant diagram (view along the PtP₂ plane) illustrates steric interactions of *trans*-stilbene with the Pt(diphos) fragment. Black circles represent steric hindrance due to substituents of the C₂-symmetric diphosphine.

Several related metal-mediated *cis*–*trans* isomerizations of stilbene and its derivatives have been reported.¹⁴

The syntheses of the stilbene complexes generally go in high yield, with lower isolated yields attributable to the high solubility of some derivatives in organic solvents. Several reducing agents were assayed, with those listed in the scheme being most convenient. For example, complexes **7** and **8** could also be prepared with LiBEt₃H, but the formation of a dark oil after extraction with toluene made separation and purification of the products difficult.

The new complexes are yellow solids (**4** is red), which are robust in solution in the absence of air and can be stored at room temperature as solids under nitrogen for months. Since *trans*-stilbene is prochiral, binding different enantiofaces of this olefin in **5**–**8** gives mixtures of diastereomers.¹⁵ The binding selectivities can be rationalized on steric grounds with a quadrant diagram analysis,⁸ as shown in Figure 2; this is also discussed below along with structural data obtained from X-ray crystallography. In most cases, recrystallization gave samples enriched in one enantiomer, and *R*-Tol-Binap derivative **6** could be isolated as a pure diastereomer (see below).

The stilbene complexes were characterized by spectroscopy (Table 2), by elemental analyses and mass spectrometry, and by X-ray crystallography (see below). The ³¹P{¹H} NMR spectra exhibit singlets with platinum satellites with ¹J_{P–Pt} values ranging from ca. 3000 to 3700 Hz, similar to those of previously reported Pt(0) complexes of ethylene.¹⁶ The olefinic protons of

Table 2. Selected NMR Data for the Complexes Pt(diphos)(*trans*-stilbene)^a

	3	4	5a,b	6a,b	7a,b	8a,b
δ (¹ H) ^b	4.88	4.35	4.93 4.90	4.65 4.62	4.64 4.45	4.25 4.15
² J _{Pt–H} ^b	61	60	63 65	64 60	61 63	59 59
δ (¹³ C) ^c	<i>d</i>	57.5	54.4 54.6	57.5 <i>d</i>	50.3 <i>d</i>	58.5 208
¹ J _{Pt–C} ^c	<i>d</i>	215	<i>d</i>	217	230	206
² J _{P–C} ^c	<i>d</i>	14	15 15	14 <i>d</i>	16 16	13 13
δ (³¹ P)	49.0	24.5	56.4 53.8	27.8 30.0	71.4 66.3	10.6 10.5
¹ J _{Pt–P}	3343	3763	3333 3316	3546 3490	3137 3091	3632 3623

^a In C₆D₆, except for the ¹³C spectrum of **4** (CD₂Cl₂). Chemical shifts are given in ppm and coupling constants in hertz. For **5**–**8**, **a** refers to the major diastereomer and **b** to the minor one. ^b Coordinated stilbene CH. ^c Coordinated stilbene CH. ^d Not measured.

coordinated *trans*-stilbene appear between 4.4 and 4.9 ppm in the ¹H NMR spectra. They exhibit coupling to ¹⁹⁵Pt with ²J_{Pt–H} of approximately 60 Hz, and the ¹³C–{¹H} NMR signals of the olefinic carbons appear as an apparent triplet (²J_{CP} = 13–16 Hz) between 50 and 59 ppm with a ¹J_{Pt–C} coupling of approximately 200 Hz.

Spectroscopic monitoring of the syntheses summarized in Scheme 1 provided more information on the formation of **5**–**8** and on the observed diastereoselectivity in their binding of *trans*-stilbene. For example, treatment of Pt((*S,S*)-chiraphos)Cl₂ with LiBEt₃H in THF gave a solution whose ³¹P NMR spectrum showed a 2:1 mixture of diastereomers. However, after extraction with toluene and one recrystallization, compounds **5a** and **5b** were obtained in an approximately equal ratio. Multiple recrystallizations from THF/petroleum ether result in enrichment (5:1) of complex **5a**. The ratio of **5a** to **5b** also changes in solution in the absence of excess *trans*-stilbene. For example, a sample of diastereomers **5a** and **5b** in C₆D₆ (5:1 ratio) converted to a 1.5:1 mixture over 2 weeks.

Treatment of Pt(*R*-Tol-binap)Cl₂ (**2**) with NaBH₄ in EtOH initially gave a dark purple reaction mixture, which turned brown over ~12 h while some of the yellow product **6** precipitated from solution. The ³¹P NMR spectrum of the purple solution shows a singlet at 28.8 ppm (¹J_{Pt–P} = 2073 Hz), which is tentatively assigned to the dihydride Pt(*R*-Tol-Binap)H₂ on the basis of its small ¹J_{Pt–P} coupling.¹⁷ In another synthesis, a different intermediate (δ 27.7, with two sets of Pt satellites, ¹J_{P–Pt} = 3114 and ³J_{P–Pt} = 174 Hz), possibly the dinuclear cation¹⁸ [Pt₂(*R*-Tol-Binap)₂H₃]⁺, was observed. Nonetheless, in both cases, after removal of the solvent under vacuum and extraction with toluene, the ³¹P NMR spectrum exhibits a 1.5:1 mixture of diastereomers **6a** and **6b**.

Recrystallization of this mixture from THF or THF/petroleum ether gives exclusively diastereomer **6a**. The mother liquor is enriched in the minor diastereomer (by ³¹P NMR), which implies that diastereomer **6a** prefer-

(14) For examples of photochemical isomerization, see: (a) Wrighton, M.; Hammond, G. S.; Gray, H. B. *J. Am. Chem. Soc.* **1971**, *93*, 3285–3287. (b) Sakaki, S.; Okitaka, I.; Ohkubo, K. *Inorg. Chem.* **1984**, *23*, 198–203. For thermal processes, see, for example: (c) Manuel, T. A. *J. Org. Chem.* **1962**, *27*, 3941–3945. (d) Castiglione, M.; Giordano, R.; Sappa, E. *J. Organomet. Chem.* **1991**, *407*, 377–389. (e) Todres, Z. V.; Ionina, E. A.; Pombeiro, A. J. L. *J. Organomet. Chem.* **1992**, *438*, C23–C25. Here, a referee suggested another plausible mechanism for isomerization, reversible protonation of the Pt complex by catalytic adventitious acid.

(15) For related observations in Ni(0) complexes of chiral diphosphines, see: Casalnuovo, A. L.; RajanBabu, T. V.; Ayers, T. A.; Warren, T. H. *J. Am. Chem. Soc.* **1994**, *116*, 9869–9882.

(16) The P–Pt coupling constants for PtL₂(C₂H₄) complexes where L = PPh₃, ¹/₂dppf, and ¹/₂dppb are 3721, 3303, and 3524 Hz, respectively. See ref 7.

(17) Schwartz, D. J.; Andersen, R. A. *J. Am. Chem. Soc.* **1995**, *117*, 4014–4025.

(18) Knobler, C. B.; Kaesz, H. D.; Minghetti, G.; Bandini, A. L.; Banditelli, G.; Bonati, F. *Inorg. Chem.* **1983**, *22*, 2324–2331.

entally crystallizes from the solution. Pure samples of **6a** slowly isomerized in solution to give mixtures of **6a** and **6b** over several days. To obtain qualitative mechanistic information on this process, the isomerization of C₆D₆ solutions of pure **6a** with 0, 1, 5, and 10 equiv of *trans*-stilbene was monitored over several days by ³¹P NMR. Isomerization occurred most quickly in the tube with no added stilbene, and increasing the concentration of stilbene slowed the isomerization. It was not possible to determine if equilibrium mixtures of **6a** and **6b** were obtained due to decomposition after several weeks. No new signals were observed in the NMR spectra of these solutions, and the ³¹P NMR chemical shifts and Pt–P coupling constants of **6a** and **6b** were unaffected by stilbene concentration. These observations suggest that isomerization of **6** occurs by a dissociative pathway involving loss of stilbene and binding of the other enantioface.¹⁹

The (*R,R*)-Me-Duphos and (*S,S*)-Diop complexes **7** and **8** were prepared using NaBH(OMe)₃ in THF. For **7**, both prior to workup and after one recrystallization from THF/MeOH, the ratio of the two diastereomers is 3:1 (**a**:**b**). As for Chiraphos analogue **5**, multiple recrystallizations (petroleum ether, –25 °C) give a sample enriched in one diastereomer (7:1 ratio). When this material was dissolved in C₆D₆, the ratio changed to 3:1 over 1 week. In the case of Diop complex **8**, the diastereomers **8a** and **8b** exist in approximately equal ratios (1.2:1) in the reaction mixture prior to workup and after two recrystallizations from petroleum ether. This ratio did not change on standing in solution.

From these observations, it appears that the kinetic diastereomer ratios are not much different from the apparent thermodynamic ones. We assume that the diastereomer ratios observed by NMR after days or weeks represent true equilibrium mixtures, but since isomerization is slow and since we have not been able to resolve both diastereomers of a given complex and allow them to reach “equilibrium” separately, this is not necessarily true. With this assumption, the observation in all cases of both diastereomers shows that they are similar in energy. Diastereomer interconversion occurs both in the presence and absence of *trans*-stilbene; qualitative observations for Tol-Binap complex **6** suggest that this isomerization is a dissociative process. As might be expected, the more rigid Tol-Binap and Duphos complexes are more effective than the relatively flexible Diop and Chiraphos ones in recognition of *trans*-stilbene enantiofaces.

Crystallographic Studies. The structures of complexes **4–6** and **8** were determined by X-ray crystallography. Data collection and structure refinement are summarized in Table 1. ORTEP diagrams are shown in Figures 3–6, selected bond lengths and angles are given in Table 3, and additional information appears in the Experimental Section and the Supporting Information. As expected from the solution NMR results, Chiraphos complex **5** crystallizes as a mixture of diastereomers but resolved *R*-Tol-Binap compound **6** exists as a single diastereomer in the solid state. Although approximately equal amounts of the diastereomers of

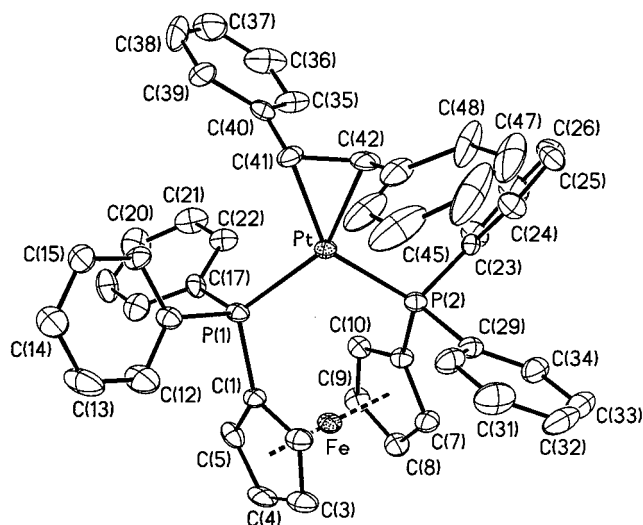


Figure 3. ORTEP diagram of **4**, with 30% probability thermal ellipsoids. The THF molecule is not shown.

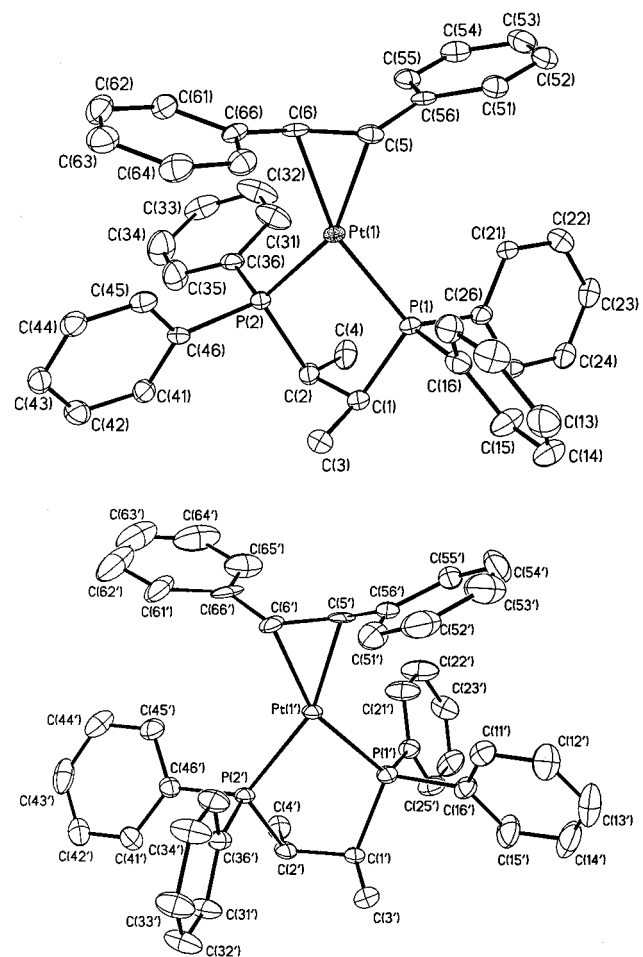


Figure 4. ORTEP diagrams of the two independent molecules of **5** in the unit cell, with 30% probability thermal ellipsoids. The THF molecules are not shown.

Diop complex **8** were observed in solution by NMR, the crystal studied contained a single diastereomer.

Despite the presence of enantiomerically pure (*S,S*)-Diop ligand in compound **8**, the Pt complex crystallizes in the centrosymmetric space group *P* $\bar{1}$ (see Experimental Section). The packing of the crystal lattice is apparently determined by the majority of the structure represented as (stilbene)Pt(Ph₂P...PPh₂). Thus, the

(19) Peng, T.-S.; Gladysz, J. A. *J. Am. Chem. Soc.* **1992**, *114*, 4174–4181.

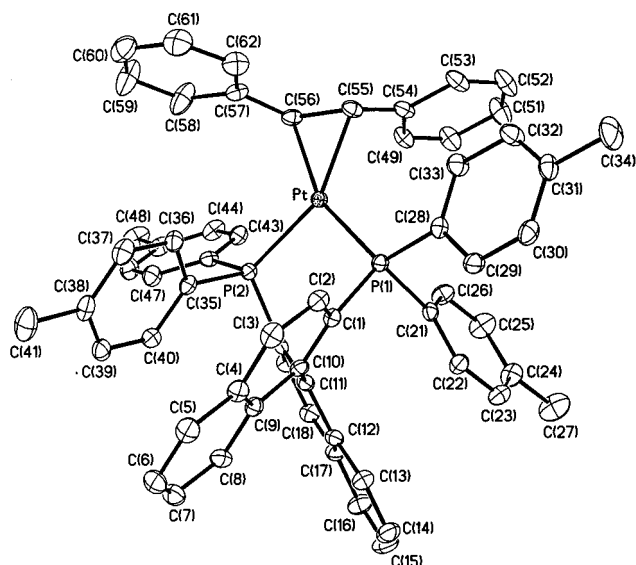


Figure 5. ORTEP diagram of **6**, with 30% probability thermal ellipsoids. The THF molecule is not shown.

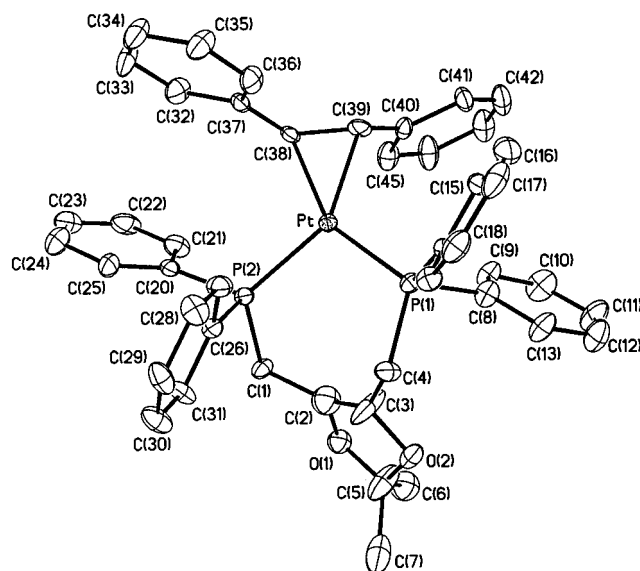


Figure 6. ORTEP diagram of **8**, with 30% probability thermal ellipsoids. The solvent molecules are not shown.

crystallographic symmetry exceeds the molecular symmetry. Consequently, the five-membered ring is equally disordered over two positions corresponding to the (*R,R*) and (*S,S*) configurations in each molecule. As pointed out by a referee, the structure of a related chiral organopalladium complex which also crystallized in $P\bar{1}$ shows similar effects and has been described as a quasiracemate.²⁰

In these complexes, the coordination geometry at platinum is trigonal and almost planar. The dihedral angles between the P–Pt–P and the C–Pt–C planes (Table 3) range from 5.8° to 11.5°. Despite steric and electronic differences between the diphosphine ligands, the Pt–P and Pt–C distances are very similar in this series, ranging from 2.261(3) to 2.290(2) Å and from 2.115(4) to 2.146(4) Å, respectively. Similarly, the C–C bond lengths in coordinated *trans*-stilbene, which range

Table 3. Selected Bond Lengths (Å) and Angles (deg) in Pt(diphos)(*trans*-stilbene) Complexes^a

	4	5	5'	6	8
Pt–P	2.261(3)	2.272(2)	2.271(2)	2.2806(9)	2.284(2)
Pt–C	2.263(3)	2.277(2)	2.274(2)	2.2840(8)	2.290(2)
C–C	1.47(2)	1.438(9)	1.449(10)	1.450(5)	1.459(10)
P–Pt–P	105.95(12)	87.13(6)	86.55(6)	94.41(3)	100.85(6)
C–Pt–C	40.5(5)	39.3(2)	39.9(3)	39.79(14)	39.8(3)
P–Pt–C	105.1(4)	115.6(2)	116.6(2)	109.48(11)	106.8(2)
	109.1(4)	118.3(2)	117.1(2)	116.67(10)	112.8(2)
	148.7(4)	157.2(2)	156.9(2)	155.83(10)	151.8(2)
(P–Pt–P)– (C–Pt–C)	11.5	8.1	5.8	8.7	8.9

^a 5 and 5' are diastereomers.

from 1.438(9) to 1.47(2) Å, do not differ significantly. As expected, these bond distances are longer than the one in the free olefin (1.341(2) Å at 113K).²¹ The C–Pt–C angles in bound stilbene (ranging from 39.3(2)° to 40.5(5)°) fall in a narrow range.

Related ethylene^{9d} (**10**) and C₆₀ (**11**)²² complexes of the Pt(Diop) fragment have been structurally characterized previously. These show larger Diop bite angles than in **8** (105.25(4)°, 109.47(13)°, and 100.85(6)°, respectively) and similar C–Pt–C angles (38.9(3)°, 42.0(4)°, and 39.8(3)°). The Pt–C distances in the fullerene complex (2.09(2) and 2.12(2) Å) are not significantly different from those in **8** (2.143(6), 2.145(6) Å), but those in the ethylene adduct (2.109(5), 2.100(5) Å) are slightly shorter. The Pt–P bond distances in **8** (2.284(2), 2.290(2) Å) are slightly longer than those in **10** (2.261(4), 2.254(1) Å) and **11** (2.262(4), 2.279(4) Å). These differences are presumably due to a combination of steric and electronic effects.

The bite angle in Tol-Binap complex **6** (94.41(3)°) is similar to the average one in Pt(Binap)₂ (**12**; 92°).²³ The Pt–P distances in **6** (2.2806(9) and 2.2840(8) Å) are shorter than those in **12** (average 2.33 Å); the latter were previously described as unusually long, perhaps due to the distortions imposed by the presence of two chelate rings in **12**. The Binap twist angle in **6** (71.5°) is similar to that in **12** (78°).

The conformational flexibility of dpfp has been reviewed.²⁴ The bite angle observed in **4** (105.95(12)°) is within the usual range of 93–112°, and the Pt–P bond lengths (2.261(3) and 2.263(3) Å) are similar to those in Pt(dpfp)Cl₂·0.5(acetone) (2.252(4) and 2.260(4) Å).²⁵

The structure of Chiraphos complex **5** allows direct comparison of the two diastereomers formed by binding the different enantiofaces of *trans*-stilbene. The data in Table 3 show that the two diastereomers have virtually identical structures in the solid state. Qualitatively, the observed small binding selectivity in solution may be ascribed to unfavorable steric repulsions

(21) Ogawa, K.; Sano, T.; Yoshimura, S.; Takeuchi, Y.; Toriumi, K. *J. Am. Chem. Soc.* **1992**, *114*, 1041–1051 and references therein.

(22) Bashilov, V. V.; Petrovskii, P. V.; Sokolov, V. I.; Dolgushin, F. M.; Yanovsky, A. I.; Struchkov, Y. T. *Izv. Akad. Nauk, Ser. Khim.* **1996**, 1268–1274.

(23) Tominaga, H.; Sakai, K.; Tsubomura, T. *J. Chem. Soc., Chem. Commun.* **1995**, 2273–2274.

(24) Gan, K.-S.; Hor, T. S. A. In *Ferrocenes. Homogeneous Catalysis, Organic Synthesis, Materials Science*; Togni, A., Hayashi, T., Eds.; VCH: Weinheim, Germany, 1995; pp 3–104.

(25) Clemente, D. A.; Pilloni, G.; Corain, B.; Longato, B.; Tiripicchio-Camellini, M. *Inorg. Chim. Acta* **1986**, *115*, L9–L11.

(20) Alcock, N. W.; Hulmes, D. I.; Brown, J. M. *J. Chem. Soc., Chem. Commun.* **1995**, 395–397. See also: Fraser, C.; Ostrander, R.; Rheingold, A. L.; White, C.; Bosnich, B. *Inorg. Chem.* **1994**, *33*, 324–337.

between the Chiraphos PPh₂ groups and the coordinated stilbene (see Figures 2 and 4). The greater face selectivity seen in Tol-Binap complex **6** is presumably due to increased steric interactions in this complex and more efficient transfer of chiral information from the ligand backbone to the PPh₂ groups.²

Conclusion

A series of platinum(0) *trans*-stilbene complexes has been prepared, and the effect of several chiral diphosphine ligands on enantioface-selective binding of the prochiral olefin was probed by NMR and X-ray crystallography. The rigidity of the chiral ligand appears to play an important role in asymmetric recognition. Further work with these compounds will focus on studies of oxidative addition and their use as catalyst precursors in asymmetric hydrophosphination.

Experimental Section

General Details. Unless otherwise noted, all reactions and manipulations were performed in dry glassware under a nitrogen atmosphere at 20 °C in a drybox or using standard Schlenk techniques. Petroleum ether (bp 38–53 °C), ether, THF, and toluene were dried and distilled before use from Na/benzophenone. CH₂Cl₂ was distilled from CaH₂. Methanol and ethanol were dried over Mg(OMe)₂ and Mg(OEt)₂, respectively.

NMR spectra were recorded on a Varian 300 MHz spectrometer. ¹H and ¹³C NMR chemical shifts are reported relative to Me₄Si and were determined by reference to the residual ¹H or ¹³C solvent peaks. ³¹P NMR chemical shifts are reported relative to H₃PO₄ (85%), used as an external reference. Unless otherwise noted, peaks in NMR spectra are singlets; coupling constants are reported in hertz. Infrared spectra, recorded as KBr pellets on a Perkin-Elmer 1600 series FTIR instrument, are reported in cm⁻¹. Elemental analyses were provided by Schwarzkopf Microanalytical Laboratory. Mass spectra were done at the University of Illinois, Urbana-Champaign, IL. Unless otherwise noted, reagents were from commercial suppliers. Pt(COD)Cl₂ was made by the literature procedure.²⁶ The Pt(diphos)Cl₂ compounds were made from Pt(COD)Cl₂ and the diphos ligand in CH₂Cl₂, as described in more detail for **1** and **2**.

Pt[(*R,R*)-Me-Duphos]Cl₂ (1**).** A solution of (*R,R*)-Me-Duphos (535 mg, 1.75 mmol) in CH₂Cl₂ (5 mL) was added dropwise to a stirring slurry of Pt(COD)Cl₂ (654 mg, 1.75 mmol) in CH₂Cl₂ (10 mL) to give a white slurry. In the air, the solvent was removed under reduced pressure and the remaining white crystals were washed with Et₂O to give Pt[(*R,R*)-Me-Duphos]Cl₂ in essentially quantitative yield. The product was recrystallized from CH₂Cl₂. ¹H NMR (CDCl₃): δ 7.67 (3-line pattern, 4H, Ar), 3.55–3.41 (m, 2H, CH), 2.78–2.65 (m, 2H, CH), 2.45–2.26 (m, 4H, CH₂), 2.26–2.06 (m, 2H, CH₂), 1.79–1.64 (m, 2H, CH₂), 1.43 (dd, ³J_{PH} = 19, ³J_{HH} = 7, 6H, Me), 0.87 (dd, ³J_{PH} = 17, ³J_{HH} = 7, 6H, Me). ¹³C{¹H} NMR (CDCl₃): δ 140.9 (dd, ¹J_{CP} = 51, ²J_{CP} = 26, quat C), 132.6–132.1 (m, Ar), 41.1 (d, ¹J_{CP} = 39, ²J_{C-Pt} = 31, CH), 36.8 (d, ¹J_{CP} = 38, ²J_{C-Pt} = 31, CH), 36.8 (³J_{C-Pt} = 33, CH₂), 35.8 (broad 2-line pattern with apparent ¹J_{CP} = 5, CH₂), 17.1 (3-line pattern, ³J_{C-Pt} = 34, Me), 13.8 (Me). ³¹P{¹H} NMR (CDCl₃): δ 69.4 (¹J_{P-Pt} = 3533). Anal. Calcd for C₁₈H₂₈P₂PtCl₂: C, 37.77; H, 4.93. Found: C, 37.97; H, 5.03.

Pt(*R-Tol-Binap*)Cl₂ (2**).** In the air, to a stirring solution of Pt(COD)Cl₂ (396 mg, 1.06 mmol) dissolved in CH₂Cl₂ (15 mL) was added *R-Tol-Binap* (718 mg, 1.06 mmol) dissolved in CH₂Cl₂ (5 mL). The pale-yellow solution was heated at

approximately 30 °C for 10 min. The solvent was removed in vacuo, and the resulting solid was washed with 3 5 mL portions of ether. Recrystallization from CH₂Cl₂/ether at –25 °C yielded 918 mg (92%) of Pt(*R-Tol-Binap*)Cl₂ in 3 crops. ¹H NMR (CDCl₃): δ 7.71–7.64 (m, 4H, Ar), 7.54–7.30 (m, 12H, Ar), 7.19–7.06 (m, 6H, Ar), 6.71 (d, 2H, Ar), 6.40 (d, 4H, Ar), 2.35 (6H, *p*-tol Me), 1.95 (6H, *p*-tol Me). ¹³C{¹H} NMR (CDCl₃): δ 141.2 (Ar), 140.9 (Ar), 138.7 (Ar), 135.6–135.5 (m, Ar), 134.9–134.4 (m, Ar), 133.9 (Ar), 133.0 (Ar), 128.9–128.7 (m, Ar), 128.4–127.8 (br m, Ar), 127.5 (Ar), 126.6 (Ar), 124.9 (Ar), 123.9 (Ar), 119.4 (Ar), 118.5 (Ar), 21.6 (*p*-tol Me), 21.3 (*p*-tol Me). ³¹P{¹H} NMR (CDCl₃): δ 10.0 (¹J_{P-Pt} = 3674). Anal. Calcd for C₄₈H₄₀P₂PtCl₂: C, 61.02; H, 4.28. Found: C, 60.93; H, 4.31.

Pt(dppe)(*trans*-stilbene) (3**).** A Schlenk tube was charged with Pt(dppe)Cl₂ (2.0 g, 3 mmol) and an excess of *trans*-stilbene (815 mg, 4.52 mmol). Addition of THF (50 mL) gave a slurry, which was treated over 5 min with 6.5 mL of a 1 M solution of LiBEt₃H in THF (6.5 mmol) to give a homogeneous orange solution after addition was complete. The THF was removed in vacuo, and the resulting yellow residue was extracted with 4 × 30 mL of toluene. The toluene was removed under vacuum, and the resulting yellow solid was recrystallized from THF/petroleum ether at –20 °C to give 1671 mg (72%) of yellow-orange solid in 4 crops. An analytical sample was recrystallized twice from THF/petroleum ether to give yellow crystals. ¹H NMR (C₆D₆): δ 7.69–7.63 (m, 4H, Ar), 7.39–7.29 (m, 6H, Ar), 7.16–6.87 (m, 20H, Ar), 4.90–4.86 (m, 2H, ²J_{Pt-H} = 61, CH=CH), 2.05–1.96 (m, 4H, CH₂). ³¹P{¹H} NMR (C₆D₆): δ 49.0 (¹J_{Pt-P} = 3343). IR: 3052, 1595, 1490, 1434, 1214, 1100, 1068, 1027, 963, 876, 815, 753, 693, 522, 494. Anal. Calcd for C₄₀H₃₆P₂Pt: C, 62.08; H, 4.70. Found: C, 61.86; H, 4.93.

Pt(dppe)(*cis*-stilbene) (9**).** Attempts to prepare this complex as for the *trans*-stilbene analogue (or using NaBH-(OMe)₃) gave a mixture of the *cis*- and *trans*-stilbene complexes as a brown powder. Monitoring of the reaction by ³¹P NMR shows that *cis*-stilbene complex **9** is initially formed and partially isomerizes to *trans*-stilbene complex **3** during workup/recrystallization. Some characteristic resonances of the *cis*-stilbene complex could be differentiated from those of the *trans* one in the mixture. ¹H NMR (C₆D₆): δ 4.98 (br, 2H, ²J_{Pt-H} = 70). ³¹P{¹H} NMR (C₆D₆): δ 50.9 (¹J_{Pt-P} = 3220).

Pt(dppf)(*trans*-stilbene) (4**).** To a solution of Pt(dppf)Cl₂ (288 mg, 0.35 mmol) in THF (5 mL) was added *trans*-stilbene (64 mg, 0.38 mmol) and 710 μL of LiBEt₃H (1 M in THF, 0.710 mmol) to afford a dark yellow solution. The solvent was removed under vacuum, and the solid residue was redissolved in toluene and filtered. The solvent was removed under vacuum, and the product was recrystallized from THF/petroleum ether to give a dark red solid, 289 mg (89% yield). X-ray-quality crystals were obtained after several additional recrystallizations from CH₂Cl₂/petroleum ether. ¹H NMR (C₆D₆): δ 7.84–7.83 (m, 4H, Ar), 7.40–7.31 (m, 8H, Ar), 7.19–6.88 (m, 18H, Ar), 4.35 (m, ²J_{Pt-H} = 60, 2H, CH=CH), 4.22 (2H, Cp), 4.11 (2H, Cp), 3.84 (2H, Cp), 3.81 (2H, Cp). ¹³C{¹H} NMR (CD₂Cl₂): δ 147.4 (quat Ar), 139.6–139.0 (m, Ar), 138.2 (Ar), 137.6 (Ar), 136.6–136.0 (m, Ar), 134.4–134.2 (m, Ar), 133.4–133.2 (m, Ar), 129.5 (Ar), 129.4 (Ar), 129.3 (Ar), 129.0 (Ar), 128.9 (Ar), 128.5 (Ar), 128.0 (m, Ar), 127.7 (br, Ar), 126.8 (Ar), 125.7–125.4 (m, Ar), 122.9 (Ar), 82.8–82.1 (m, Cp), 74.9–74.4 (m, Cp), 71.8 (Cp), 71.4 (Cp), 57.5 (¹J_{Pt-C} = 215, ²J_{PC} = 14, CH=CH). ³¹P{¹H} NMR (C₆D₆): δ 24.5 (¹J_{Pt-P} = 3763). IR: 3053, 3022, 2924, 1596, 1491, 1431, 1096, 1028, 743, 694. Anal. Calcd for C₄₈H₄₀P₂FePt: C, 62.01; H, 4.34. Found: C, 62.01; H, 4.25.

Pt((*S,S*)-Chiraphos)(*trans*-stilbene) (5**).** To a stirring slurry of Pt((*S,S*)-Chiraphos)Cl₂ (280 mg, 0.404 mmol) and *trans*-stilbene (109 mg, 0.607 mmol) in THF (10 mL) was added LiBEt₃H (849 μL of 1 M THF solution, 0.849 mmol). The reaction mixture immediately turned dark yellow and was allowed to stir at room temperature for 5 h. The solvent was

(26) McDermott, J. X.; White, J. F.; Whitesides, G. M. *J. Am. Chem. Soc.* **1976**, *98*, 6521–6528.

removed in vacuo, and the dark yellow residue was extracted with toluene (20 mL). The toluene solution was filtered, and the filtrate was concentrated under vacuum to approximately 5 mL. Cooling of this solution to $-25\text{ }^{\circ}\text{C}$ overnight gave 180 mg (56%) of a pale yellow product, an approximately equal mixture of diastereomers. From the mother liquor, the solvent was removed in vacuo and the resulting residue was dissolved in a minimum amount of THF. This solution was filtered, petroleum ether was added, and the solution was cooled to $-25\text{ }^{\circ}\text{C}$ to give a second crop (47 mg, 15%; total yield = 227 mg, 71%). Multiple recrystallizations from THF/petroleum ether at $-25\text{ }^{\circ}\text{C}$ gave crystals suitable for X-ray diffraction. The NMR spectra are reported as a mixture of diastereomers (**a** and **b**) unless otherwise indicated. ^1H NMR (C_6D_6): δ 7.92–7.86 (m, 4H, Ar), 7.48–7.18 (m, 20H, Ar), 7.13–6.97 (m, 6H, Ar), 4.93 (m, $^2J_{\text{Pt-H}} = 63$, 2H, CH=CH, **a**), 4.90 (m, $^2J_{\text{Pt-H}} = 65$, 2H, CH=CH, **b**), 2.51–2.40 (m, 2H, CHMe, **a**), 2.34–2.27 (m, 2H, CHMe, **b**), 0.76 (dd, $^3J_{\text{PH}} = 11$, $^3J_{\text{HH}} = 6$, 6H, CHMe, **b**), 0.67 (dd, $^3J_{\text{PH}} = 12$, $^3J_{\text{HH}} = 6$, 6H, CHMe, **a**). $^{13}\text{C}\{^1\text{H}\}$ NMR (C_6D_6): δ 149.6 (quat Ar), 136.1–135.4 (m, Ar), 133.9–133.4 (m, Ar), 130.8 (Ar), 130.5 (Ar), 130.0 (Ar), 129.3–128.6 (m, Ar), 126.9 (Ar), 123.4 (Ar), 54.6 (apparent t, $^2J_{\text{CP}} = 15$, **b**), 54.4 (apparent t, $^2J_{\text{CP}} = 15$, **a**), 42.7–40.7 (m, CHMe), 18.2 (CHMe, **a**), 17.6 (CHMe, **b**). $^{31}\text{P}\{^1\text{H}\}$ NMR (C_6D_6): δ 56.4 ($^1J_{\text{P-Pt}} = 3333$, **a**), 53.8 ($^1J_{\text{P-Pt}} = 3316$, **b**). IR: 3044, 2966, 1595, 1488, 1427, 1211, 1094, 1066, 1022, 744, 688, 633, 533. Low-resolution FAB MS (3-NBA): m/z 815.1, 802.1 (MH^+), 621.0 [(MH – PhCH=CHPh) $^+$], 565.0, 544.0, 485.9, 408.9, 332.9, 301.9, 183.0, 154.1. High-resolution FAB-MS (3-NBA) m/z found 802.2335, calcd for $\text{C}_{42}\text{H}_{41}\text{P}_2^{195}\text{Pt}$ 802.2331. Anal. Calcd for $\text{C}_{42}\text{H}_{40}\text{P}_2\text{-Pt}$: C, 62.91; H, 5.04. Found: C, 62.14; H, 5.44.

Pt(*R*-Tol-Binap)(*trans*-stilbene) (6). Pt(*R*-Tol-Binap)Cl₂ (313 mg, 0.331 mmol) and *trans*-stilbene (179 mg, 1.00 mmol) were dissolved in EtOH (15 mL) and THF (5 mL). Sodium borohydride (50 mg, 1.33 mmol) was dissolved in EtOH (10 mL) and transferred to the stirring reaction mixture via cannula. The reaction mixture immediately became dark purple and was allowed to stir overnight at room temperature. The solvent was removed in vacuo, and the dark yellow residue was extracted with toluene (30 mL) and filtered. The toluene was removed in vacuo, and the yellow solid was dissolved in THF and filtered. Petroleum ether was added to the THF solution, and cooling to $-25\text{ }^{\circ}\text{C}$ gave 227 mg (65%) of a single diastereomer (**a**) by NMR. ^1H NMR (C_6D_6): δ 8.11–8.04 (m, 4H, Ar), 7.56–7.50 (m, 2H, Ar), 7.29–7.13 (m, 14H, Ar), 6.95–6.65 (m, 14H, Ar), 6.09–6.06 (m, 4H, Ar), 4.65 (m, $^2J_{\text{Pt-H}} = 64$, 2H, CH=CH), 2.13 (6H, tol Me), 1.64 (6H, tol Me). $^{13}\text{C}\{^1\text{H}\}$ NMR (C_6D_6): δ 149.2 (quat Ar), 148.2 (quat Ar, $J_{\text{C-Pt}} = 48$), 140.2 (Ar), 139.4 (Ar), 138.6–138.1 (m, Ar), 137.3 (Ar), 137.1 (Ar), 136.8 (Ar), 135.8–135.6 (m, Ar), 134.8–134.4 (m, Ar), 133.8 (Ar), 132.7 (Ar), 132.0 (Ar), 126.1 (Ar), 125.7 (Ar), 123.2 (Ar), 57.5 (apparent t, $^2J_{\text{CP}} = 14$, $^1J_{\text{C-Pt}} = 217$, CH=CH), 21.6 (tol Me), 21.3 (tol Me). $^{31}\text{P}\{^1\text{H}\}$ NMR (C_6D_6): δ 27.8 ($^1J_{\text{P-Pt}} = 3546$). IR: 3022, 1588, 1494, 1444, 1394, 1305, 1211, 1183, 1094, 1066, 1022, 861, 805, 744, 694, 633, 611, 505, 466, 427. Low-resolution FAB MS (3-NBA): m/z 1092.3, 1071.1, 1054.2 (MH^+), 1040.2, 1026.2, 1010.2, 995.2, 980.2, 873.1 [(MH – PhCH=CHPh) $^+$], 763.4, 465.1, 307.0, 154.1. High-resolution FAB MS (3-NBA) m/z found 1054.3281, calcd for $\text{C}_{62}\text{H}_{53}\text{P}_2\text{-}^{195}\text{Pt}$ 1054.3270. Anal. Calcd for $\text{C}_{62}\text{H}_{52}\text{P}_2\text{-Pt}\cdot\text{THF}$: C, 70.37; H, 5.38. Found: C, 70.05; H, 5.62. The presence of THF was confirmed by ^1H NMR.

Some characteristic resonances of the minor diastereomer (**b**) could be differentiated from those of the major one (**a**) in the crude product. ^1H NMR (C_6D_6): δ 4.62 (m, $^2J_{\text{Pt-H}} = 60$, 2H, CH=CH), 2.09 (6H, *p*-tol Me), 1.71 (6H, *p*-tol Me). $^{31}\text{P}\{^1\text{H}\}$ NMR (C_6D_6): δ 30.0 ($^1J_{\text{P-Pt}} = 3490$).

Isomerization of 6. Pure samples of diastereomer **6a** (~10 mg, 0.009 mmol) were prepared in C_6D_6 with 0, 1, 5, and 10 mol equiv of *trans*-stilbene, respectively. The tubes were maintained at ambient temperature, and the isomerization of

6a to **6b** was monitored by ^{31}P NMR. After 1 day, traces of **6b** were observed. After 3 days, the ratios of **6a:6b** were 2:1, 2.5:1, 6:1, and 5:1, respectively. After 1 week, these ratios were 1.4:1, 1.8:1, 4.6:1, and 5:1. After 3 weeks, the ratio was approximately 2:1 in all four tubes but some decomposition was evident.

Pt((*R,R*)-Me-Duphos)(*trans*-stilbene) (7). To a stirring slurry of Pt((*R,R*)-Me-Duphos)Cl₂ (310 mg, 0.588 mmol) and *trans*-stilbene (116 mg, 0.644 mmol) in THF (10 mL) was added NaBH(OMe)₃ (225 mg, 1.76 mmol) dissolved in THF (5 mL). The reaction mixture immediately turned yellow, and gas was evolved. After stirring at room temperature overnight, the solvent was removed in vacuo and the yellow residue was extracted with toluene (30 mL) and filtered. The toluene was removed in vacuo, and the bright yellow solid was dissolved in a minimum amount of THF. Methanol (30 mL) was added to the THF solution, and recrystallization at $-60\text{ }^{\circ}\text{C}$ gave 200 mg (50%) of a 3:1 (**a:b**) mixture of diastereomers in three crops. The NMR spectra are reported as a mixture of diastereomers unless otherwise indicated. ^1H NMR (C_6D_6): δ 7.39–7.20 (m, 10H, Ar), 6.98–6.84 (m, 4H, Ar), 4.64 (m, $^2J_{\text{Pt-H}} = 61$, 2H, CH=CH, **a**), 4.45 (m, $^2J_{\text{Pt-H}} = 63$, 2H, CH=CH, **b**), 2.69–2.18 (m, 2H, CH), 1.97–1.89 (m, 2H, CH), 1.78–1.69 (m, 2H, CH₂), 1.59–1.52 (m, 2H, CH₂), 1.48–1.34 (m, 2H, CH₂), 1.28 (dd, $^3J_{\text{PH}} = 20$, $^4J_{\text{HH}} = 7$, 6H, Me, **a**), 1.22–1.12 (m, 2H, CH₂), 0.58 (dd, $^3J_{\text{PH}} = 14$, $^4J_{\text{HH}} = 7$, 6H, Me, **b**), 0.47 (dd, $^3J_{\text{PH}} = 20$, $^4J_{\text{HH}} = 7$, 6H, Me, **b**), 0.34 (dd, $^3J_{\text{PH}} = 14$, $^4J_{\text{HH}} = 7$, 6H, Me, **a**). $^{13}\text{C}\{^1\text{H}\}$ NMR (C_6D_6): δ 150.4–150.2 (m, quat Ar), 148.0–147.1 (m, quat Ar), 138.1 (quat Ar), 133.5–133.3 (m, Ar), 129.9 (Ar), 129.4 (Ar), 129.2 (Ar), 128.1 (Ar), 127.3 (Ar), 126.5 (Ar), 125.8–125.5 (m, Ar), 122.5 (Ar), 53.4 (apparent t, $^2J_{\text{CP}} = 16$, CH=CH, **b**), 50.3 (apparent t, $^2J_{\text{CP}} = 16$, $^1J_{\text{C-Pt}} = 230$, CH=CH, **a**), 40.9 (apparent t, $J_{\text{CP}} = 14$, CH, **b**), 39.5 (apparent t, $J_{\text{CP}} = 14$, CH, **b**), 38.4 (apparent t, $J_{\text{CP}} = 14$, CH, **a**), 37.4 (apparent t, $J_{\text{CP}} = 14$, CH, **a**), 37.2 (CH₂, **b**), 36.9 (CH₂, **a**), 36.7 (CH₂, **b**), 36.6 (CH₂, **a**), 20.3 (apparent t, $J_{\text{CP}} = 9$, $^3J_{\text{C-Pt}} = 40$, Me, **a**), 17.1 (apparent t, $J_{\text{CP}} = 9$, Me, **b**), 15.4 (Me, **b**), 15.2 (Me, **a**). $^{31}\text{P}\{^1\text{H}\}$ NMR (C_6D_6): δ 71.4 ($^1J_{\text{P-Pt}} = 3137$, **a**), 66.3 ($^1J_{\text{P-Pt}} = 3091$, **b**). IR: 3055, 2922, 2855, 1594, 1488, 1444, 1372, 1322, 1244, 1205, 1155, 1100, 1061, 1022, 994, 916, 816, 750, 694, 644, 622, 527, 500. Low-resolution FAB MS (3-NBA) m/z 682.1 (MH^+), 638.1, 547.1, 517.1, 501.1 [(MH – PhCH=CHPh) $^+$], 417.0, 360.9, 334.9, 307.0, 289.0, 180.1, 165.1, 154.1, 136.0, 120.0. High-resolution FAB MS (3-NBA) m/z found 682.2333, calcd for $\text{C}_{32}\text{H}_{41}\text{P}_2^{195}\text{Pt}$ 682.2331. Anal. Calcd for $\text{C}_{32}\text{H}_{40}\text{P}_2\text{-Pt}$: C, 56.37; H, 5.93. Found: C, 56.06; H, 6.08.

Pt((*S,S*)-Diop)(*trans*-stilbene) (8). To a stirring slurry of Pt((*S,S*)-Diop)Cl₂ (496 mg, 0.649 mmol) and *trans*-stilbene (117 mg, 0.649 mmol) in THF (10 mL) was added NaBH(OMe)₃ (194 mg, 1.52 mmol) in THF (5 mL). The reaction mixture immediately became yellow and homogeneous, and the evolution of gas was apparent. The solution was allowed to stir at room temperature for 30 min. The solvent was removed under vacuum, and the brown residue was extracted with 30 mL of toluene. The solution was filtered, and the toluene was removed in vacuo. The light brown residue was washed with 10 mL of petroleum ether, and the resulting brown solution was refrigerated at $-25\text{ }^{\circ}\text{C}$. The remaining solid was dissolved in THF and filtered. Petroleum ether was added, and cooling of this solution overnight at $-25\text{ }^{\circ}\text{C}$ gave a dark brown solid which, by ^{31}P and ^1H NMR, was a mixture of Pt((*S,S*)-Diop)-(*trans*-stilbene) and unknown impurities. From the mother liquor, the solvent was removed under vacuum to give 203 mg (34%) of the desired product. An additional 81 mg (14%, total yield = 48%) was obtained by recrystallization from the petroleum ether wash at $-25\text{ }^{\circ}\text{C}$. Recrystallization of this sample from petroleum ether at room temperature gave yellow crystals. The NMR spectra are reported as a mixture of diastereomers unless otherwise indicated. ^1H NMR (C_6D_6): δ 7.69–7.62 (m, 2H, Ar), 7.37–7.24 (m, 8H, Ar), 7.17–6.93 (m, 20H, Ar), 4.25 (m, $^2J_{\text{Pt-H}} = 59$, 2H, CH=CH, **b**), 4.15 (m, $^2J_{\text{Pt-H}}$

= 59, 2H, CH=CH, **a**), 4.10–4.08 (m, 2H, CH, **b**), 3.98–3.92 (m, 2H, CH, **a**), 3.57–3.21 (m, 2H, CH₂), 2.33–2.19 (m, 2H, CH₂), 1.19 (6H, Me, **b**), 1.18 (6H, Me, **a**). ¹³C{¹H} NMR (C₆D₆): δ 147.6–147.5 (m, quat Ar), 140.0 (apparent t, *J*_{CP} = 24, quat Ar), 138.1 (quat Ar), 137.8 (quat Ar), 137.6 (quat Ar), 137.5 (quat Ar), 134.6–134.3 (m, Ar), 134.0–133.5 (m, Ar), 132.0 (apparent t, *J*_{CP} = 7, Ar), 131.5 (apparent t, *J*_{CP} = 6, Ar), 130.4 (Ar), 129.4–128.2 (m, Ar), 127.3 (Ar), 126.5–126.0 (m, Ar), 123.6–123.4 (m, Ar), 108.6 (CMe₂, **a**), 108.4 (CMe₂, **b**), 80.1 (apparent t, *J*_{CP} = 8, CH, **b**), 79.8 (apparent t, *J*_{CP} = 8, CH, **a**), 58.6 (apparent t, *J*_{CP} = 13, ¹*J*_{Pt–C} = 208, CH=CH, **b**), 58.5 (apparent t, *J*_{CP} = 13, ¹*J*_{Pt–C} = 206, CH=CH, **a**), 36.9 (apparent t, *J*_{CP} = 13, CH₂, **a**), 35.4 (apparent t, *J*_{CP} = 13, CH₂, **b**), 27.5 (CMe₂, **a**), 27.4 (CMe₂, **b**). ³¹P{¹H} NMR (C₆D₆): δ 10.6 (¹*J*_{P–Pt} = 3632, **a**), 10.5 (¹*J*_{P–Pt} = 3623, diastereomer **b**). IR (KBr): 3433, 3051, 2983, 2932, 1595, 1489, 1433, 1372, 1243, 1215, 1159, 1098, 1044, 998, 980, 887, 816, 786, 739, 694, 507. Low-resolution FAB MS (MB): *m/z* 913.4, 879.2, 863.2, 846.3, 829.2, 756.2, 725.2, 692.2 [(MH – PhCH=CHPh)⁺], 633.2, 565.1, 531.2, 473.2, 379.1, 302.0, 271.1, 201.1. Anal. Calcd for C₄₅H₄₄O₂P₂Pt: C, 61.84; H, 5.09. Found: C, 62.46; H, 5.72.

Crystallographic Structure Determinations for 1, 4, 5, 6, and 8. The single-crystal X-ray diffraction experiments were performed on a Siemens P4/CCD diffractometer for **1**, **5**, **6**, and **8** and on a Siemens P4 diffractometer for **4**.

The systematic absences in the diffraction data were consistent for the reported space groups. For **5**, the space group *I*222 was chosen based on the combined figure of merit and the chemically reasonable and computationally stable results of refinement. For **8**, the *E*-statistics strongly suggested the centrosymmetric space group *P* $\bar{1}$, which yielded chemically reasonable and computationally stable results of refinement. Given the stated enantiomeric purity of the ligand (Strem, 99.5%), solution and refinement in *P*1 was also explored. However, despite considerable dampening and constraint, the two “independent” molecules were highly correlated and normally narrowly ranged parameters such as C–C distances in phenyl rings differed by 0.4 Å. Additionally, the methyl groups could not be located from difference maps. In **8**, atoms C(2), O(1), and C(6) are equally disordered between two positions each and were refined isotropically. See the text for further discussion.

All structures were solved using direct methods, completed by subsequent difference Fourier synthesis, and refined by full-matrix least-squares procedures. The empirical absorption corrections for **1**, **5**, and **8** were applied by using the program DIFABS.²⁷ The asymmetric units of the structures contain the following solvate molecules along with one molecule of the metal complex (two independent molecules of a metal complex in the case of **5**): **1**, a dichloromethane molecule; **4**, one THF molecule; **5**, one THF molecule in a general position and two one-half molecules of THF on 2-fold axes; **6**, one THF molecule; **8**, a complex mixture of hydrocarbons present in petroleum ether forming what appears to be a continuous hydrocarbon chain located in channels of the structure. All other non-hydrogen atoms were refined with anisotropic displacement coefficients. The hydrogen atoms in the case of the two THF molecules occupying 2-fold axes in structure **5**, in the case of the chain, and on atoms C(1) and C(3) in structure **8** were ignored. All assigned hydrogen atoms were treated as idealized contributions.

All software and sources of the scattering factors are contained in the SHELXTL (version 5.03) program library (G. Sheldrick, Siemens XRD, Madison WI).

Acknowledgment. We thank Dartmouth College, the donors of the Petroleum Research Fund, administered by the American Chemical Society, the NSF CAREER Program, the Exxon Education Foundation, and DuPont for partial support. M.A.Z. acknowledges GAANN fellowship support from the Department of Education. The University of Delaware acknowledges the NSF for their support of the purchase of the CCD-based diffractometer (grant No. CHE-9628768).

Supporting Information Available: Tables of crystal data and structure refinement, atomic coordinates, bond lengths and angles, anisotropic displacement coefficients, and H-atom coordinates for **1**, **4–6**, and **8** (42 pages). Ordering information is given on any current masthead page.

OM971000J

(27) Walker, N.; Stuart, D. *Acta Crystallogr.* **1983**, *A39*, 158.